An Efficient Two-Dimensional Graded Mesh Finite-Difference Time-Domain Algorithm for Shielded or Open Waveguide Structures

Veselin J. Brankovic, Dragan V. Krupezevic, and Fritz Arndt, *Senior Member, IEEE*

Abstract—**A finite-difference time-domain (FD-TD) algorithm is described for the efficient full-wave analysis of a comprehensive class of millimeter-wave and optical waveguide structures. The FD-TD algorithm is based on a two-dimensional graded mesh combined with adequately formulated absorbing boundary conditions. This allows the inclusion of nearly arbitrarily shaped, fully or partially lateral open or shielded guiding structures with or without layers of finite metallization thickness. Moreover, lossy dielectrics and/or lossy conductors are included in the theory. The algorithm leads to a significant reduction in cpu time and storage requirements as compared with the conventional three-dimensional eigenvalue FD-TD mesh formulation. Dispersion characteristic examples are calculated for structures suitable for usual integrated circuits, such as insulated image guides, ridge guides, dielectric waveguides, trapped image guides, coplanar-lines and microstrip lines. The theory is verified by comparison with results obtained by other methods.**

I. Introduction

SHIELDED, open or partially open waveguide structures of the class shown in Fig. 1 have found increasing interest for integrated circuit applications in the millimeter-wave and optical frequency range [1]–[17]. As this class includes a wide variety of specially shaped waveguiding structures used, in the design of integrated circuits, it is highly desirable to dispose of a reliable computer analysis which is sufficiently general and flexible to allow dominant and higher-order mode solutions of all desired cases including open or partially open structures.

Various methods of analyzing one or several of the structures of Fig. 1 have been the subject of many papers, including different kinds of mode-matching techniques [1]–[10], [13], the finite-element method [11], the finite-difference frequency-domain method [12], [14], [15], and, more recently, the finite-difference time-domain (FD-TD) method [18]–[28]. As for the criteria of flexibility, accuracy and computational efficiency, the FD-TD method is considered to be a very appropriate candidate for solving the waveguide eigenvalue problems with particular cross-sectional shapes, such as those shown in Fig. 1. The conventional FD-TD approach, however, utilizes a three-dimensional Yee's mesh for appropriate resonating sections which may be obtained by placing shorting planes along the axis of propagation of the structure under investigation. By repeating the calculation of the resonant frequency of these resonators for different distances of the shorting planes, the dispersion characteristic is then determined step by step. Consequently, the conventional approach requires considerable cpu time, needs a relatively large memory size, and tends to inaccuracies in the near of the cutoff frequencies.

A new two-dimensional FD-TD formulation has been introduced very recently [30] which helps to alleviate the above mentioned shortcomings of the conventional FD-TD approach, similar to [29], [33] where a 2-D TLM analysis has been described. Although many similarities exist between the TLM and the FD-TD method, cf. e.g.

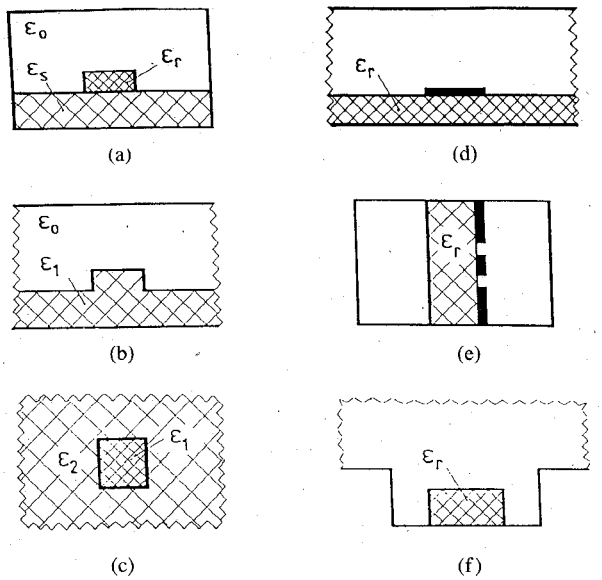

Fig. 1. The class of shielded, partially or fully open millimeter-wave and optical waveguide structures investigated with the new 2-D FD-TD method. (a) Shielded insulated image guide. (b) Lateral open ridge guide. (c) Open dielectric waveguide. (d) Lateral open microstrip line. (e) Coplanar line. (f) Open trapped image guide.

Manuscript received March 31, 1992; revised July 27, 1992.

The authors are with the Microwave Department, University of Bremen Kufsteiner Str., NW1, D-2800 Bremen, Germany.

IEEE Log Number 9203677.

[17], [31], the new 2-D FD-TD approach has the advantage of being nearly an order of magnitude faster than the 2-D TLM method. Moreover, the numerical difficulties in the field simulation in the vicinity of conductive edges reported in [32] for the classical TLM condensed node formulation (which is used also in [29], [33]) are inherently avoided by the 2-D FD-TD formulation presented in this paper.

The purpose of this paper is to extend the two-dimensional FD-TD method introduced in [30] by involving adequate absorbing boundary conditions, a graded mesh algorithm and an efficient calculation procedure for lossy structures. The inclusion of absorbing boundary conditions allows a simple, flexible, and versatile FD-TD solution for analyzing the complete class of shielded, partially or fully open waveguide structures of Fig. 1. The graded mesh permits the investigation of structures with realistic dimensions by making the mesh finer in regions of particular interest. Losses are an important factor in modern circuit design. Numerical results will be presented to elucidate the usefulness of the method. The theory is verified by comparison with results available from other methods.

II. Theory

A. Two-Dimensional FD-TD Mesh Formulation

The usual FD-TD method is formulated by discretizing Maxwell's curl equations over a finite volume and approximating the derivatives with centered difference approximations. This leads to the known three-dimensional Yee's mesh [18] in various modifications [19]–[28].

In order to derive the new two-dimensional FD-TD mesh formulation, we utilize the relationships between the transverse fields $\vec{E}_t$ and $\vec{H}_t$ of a guided wave travelling in $+z$ direction (Fig. 2)

$$\vec{E}_t(z \pm \Delta l) = \vec{E}_t(z) \cdot e^{\mp j\beta\Delta l}$$

$$\vec{H}_t(z \pm \Delta l) = \vec{H}_t(z) \cdot e^{\mp j\beta\Delta l}. \quad (1)$$

By applying Yee's formulations, e.g. in the form of [21] for anisotropic structures, a set of FD-TD equations for the six components $\vec{H}$ and $\vec{E}$ is then derived. The result is shown for H_x as an example,

$$H_x^{n+1/2}(i, j + 1/2) = H_x^{n-1/2}(i, j + 1/2) + s/[\mu_{xx}(i, j + 1/2) \cdot Z_{F0}] \cdot \{E_y^n(i, j + 1/2) \cdot [e^{-j\beta\Delta l} - 1] + E_z^n(i, j) - E_z^n(i, j + 1)\}, \quad (2)$$

where the stability factor is $s = c\Delta t/\Delta w$ with $\Delta w = \Delta x = \Delta y = \Delta l$, c is the velocity of light, Z_{F0} is the characteristic impedance of free space, and μ_{xx} is the diagonal element of the relative permeability tensor. The condition for stability in free space for a uniform mesh is $s \leq 1/\sqrt{3}$ [21]. The remaining finite difference equations related to the other five field components can be similarly calculated.

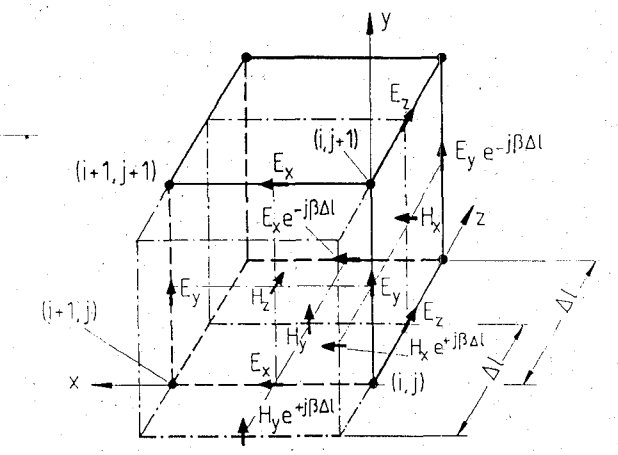

Fig. 2. New two-dimensional FD-TD mesh (i, j) for solving 2-D eigenvalue problems of waveguiding structures.

B. FD-TD Formulation of the Absorbing Boundary Conditions

For simplification, the equations of the boundary conditions are given only for the x-direction. In y-direction, the equations may be found analogously. Following Mur [20], we assume that the mesh is located in the region $x \geq 0$, that the boundary conditions are given for the plane $x = 0$, and that the outgoing wave has normal incidence. We then obtain the approximation for the boundary condition which would determine each field component W on the outer surface. This is consistent with an outgoing wave (i.e. this is absorbed), in the following form [20]:

$$\left(\partial_x - \frac{\partial_t}{v_{px}}\right) W\Big|_{x=0} = 0, \quad (3)$$

where v_{px} is the phase velocity in x-direction.

The finite-difference formulation of (3) may be written in terms of the tangential electrical field components in the subregions 1) (outer region), and 2) (mesh region) as

$$E_{1t}^{n+1} = E_{2t}^n + \frac{v_{px}\Delta t - \Delta x}{v_{px}\Delta t + \Delta x}(E_{2t}^{n+1} - E_{1t}^n). \quad (4)$$

For the graded mesh, the following approximation of equation (4) is used

$$E_{1t}^{n+1} = E_{2t}^n + \frac{s_{xloc} - \sqrt{\epsilon_{xloc}}}{s_{xloc} + \sqrt{\epsilon_{xloc}}}(E_{2t}^{n+1} - E_{1t}^n), \quad (5)$$

where s_{xloc} is the local stability factor $s_{xloc} = c\Delta t/(\Delta w \cdot p_{loc})$, with the local graded mesh scaling factor p_{loc}, and where ϵ_{xloc} is the local relative premittivity in x-direction.

C. Graded Mesh Algorithm

In order to improve the computational efficiency, a graded mesh has turned out to be very advantageous [26]. This is particularly true for open structures where, if necessary, the enclosing absorbing boundary box is made suf-

ficiently large so that the conditions mentioned above may be adequately satisfied. The basic structure of the FD-TD equations is similar to that of the uniform mesh with the exception that the uniform mesh parameters $\Delta w = \Delta x = \Delta y = \Delta l$ are replaced by $\Delta x = p\Delta w$, $\Delta y = q\Delta w$, $\Delta l = r\Delta w$, with the graded mesh scaling factors p, q, r.

With these relations, the set of FD-TD equations for the six components $\vec{H}$ and $\vec{E}$ is given in the form (e.g. for H_x) of

$$H_x^{n+1/2}(i, j + 1/2) = H_x^{n-1/2}(i, j + 1/2) + s/[\mu_{xx}(i, j + 1/2) \cdot Z_{F0}] \cdot \left\{ \frac{1}{r} E_y^n(i, j + 1/2) \cdot [e^{-j\beta\Delta l} - 1] + \frac{1}{q} [E_z^n(i, j) - E_z^n(i, j + 1)] \right\}. \quad (6)$$

In order to maintain numerical convergence, the stability factor has to be chosen on the basis of the smallest mesh parameter. To ensure continuity of fields across the interfaces between coarse and fine meshes, space averaging [28] is applied.

D. FD-TD Formulation for Lossy Structures

For deriving the FD-TD equations for lossy structures, two approaches are possible: The first approach differs between a) lossy dielectric regions (with the conductivity $\sigma_D << \omega\epsilon$) and b) lossy metal regions (with the finite conductivity $\sigma_M >> \omega\epsilon$). 2) The second, more general approach includes both cases simultaneously. In our calculations we used the general approach which has the advantage that only one formulation is necessary for the whole lossy structure.

By applying the Maxwell equations and Yee's formulations, we obtain for the component E_y, as an example:

a) In the case of a lossy dielectric region ($\sigma_D << \omega\epsilon$):

$$E_y^{n+1}(i, j + 1/2) = \left[1 - \frac{\Delta t}{\epsilon_0} \frac{\sigma_D(i, j + 1/2)}{\epsilon_{ry}(i, j + 1/2)}\right] \cdot E_y^n(i, j + 1/2) + \frac{s}{\epsilon_{ry}(i, j + 1/2)} \cdot Z_{F0} \cdot DH, \quad (7)$$

where

$$DH = \frac{H_x^{n+1/2}(i, j + 1/2)[1 - e^{j\beta\Delta l}]}{r} - \frac{H_z^{n+1/2}(i + 1/2, j + 1/2) - H_z^{n+1/2}(i - 1/2, j + 1/2)}{p},$$

and $\Delta x = p\Delta w$, $\Delta y = q\Delta w$, $\Delta l = r\Delta w$, s: stability factor, $\epsilon = \epsilon_r\epsilon_0$.

b) In the case of a lossy metallic region ($\sigma_M >> \omega\epsilon$):

$$E_y^{n+1}(i, j + 1/2) = -E_y^n(i, j + 1/2) + \frac{2}{\Delta w\sigma_M(i, j + 1/2)} \cdot DH. \quad (8)$$

The more general approach is obtained, assuming

$$E_y^{n+1/2}(i, j + 1/2) = \tfrac{1}{2}[E_y^{n+1}(i, j + 1/2) + E_y^n(i, j + 1/2)],$$

by the following equation where σ denotes the finite conductivity for lossy dielectric or metall regions

$$E_y^{n+1}(i, j + 1/2) = \frac{1 - \frac{\Delta t}{2\epsilon_0} \cdot \frac{\sigma(i, j + 1/2)}{\epsilon_{ry}(i, j + 1/2)}}{1 + \frac{\Delta t}{2\epsilon_0} \cdot \frac{\sigma(i, j + 1/2)}{\epsilon_{ry}(i, j + 1/2)}} \cdot E_y^n(i, j + 1/2) + \frac{\frac{sZ_{F0}}{\epsilon_{ry}(i, j + 1/2)}}{1 + \frac{\Delta t}{2\epsilon_0} \cdot \frac{\sigma(i, j + 1/2)}{\epsilon_{ry}(i, j + 1/2)}} \cdot DH. \quad (9)$$

The attenuation factor α of lossy structures is then calculated via the quality factor by using the equations already outlined in [33]. For the determination of the quality factor, however, an exponential regression procedure is used, i.e., for the corresponding resonance frequency, the envelope of the signal curve is evaluated by integration over several time periods. This yields high accuracy.

The principal numerical calculation steps in the two-dimensional FD-TD algorithm are similar to those in the conventional FD-TD approach with the exception that a propagation factor β has to be selected first (the choices of ß are indicated in the figure legends). After launching an excitation pulse, waiting until the distribution of the pulse is stable and performing the Fourier transformation, the modal frequencies related to the selected propagation factor are obtained. The mesh for the pulse propagation iteration needs only to be built up in the cross section x, y dimension, the number of nodes in z direction is reduced to ± 1. Also it should be emphasized that the amplitudes of all field components in the new formulation are complex quantities.

III. Results

Good agreement between our 2-D FD-TD dispersion results and those of the FD-frequency domain method [14] may be observed in Fig. 3 for the shielded insulated image guide. Fig. 4 shows the dispersion curves for different permittivities for the lateral open dielectric ridge guide. The results of the FD-TD method for a relatively low distance of the absorbing boundaries $a = 5$ h (i.e. only 2 h distance from the ridge) compare well with those obtained by the FD frequency domain method [14] for the shielded

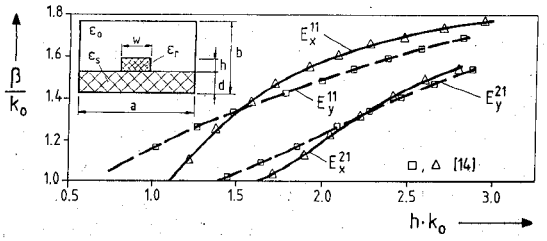

Fig. 3. Shielding insulated image guide. $w/h = 2.25$, $d/h = 0.5$, $a/h = 13.5$, $b/h = 8$, $\epsilon_r = 3.8$, $\epsilon_s = 1.5$. discretization: 54 × 64. Number of iterations $N_i = 1000$. Comparison with the FD frequency domain method [14]. (Choice of the propagation constant: $\beta = 0.5/h \cdots 5/h$, in e.g. 20 intermediate steps.)

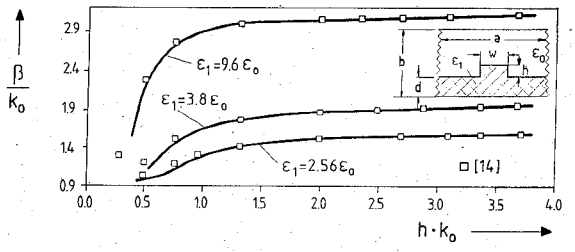

Fig. 4. Lateral open dielectric ridge guide. $w/h = 2$, $d/h = 1$, $b/h = 6$. Discretization: 60 × 72. Number of iterations $N_i = 2000$. Distance of the absorbing boundaries $a = 5$ h. Comparison with the FD frequency domain method [14] for the shielded dielectric ridge guide, lateral shield distance $a = 100$ h. (Choice of the propagation constant: $\beta = (0.3\sqrt{\epsilon_r})/\text{h} \cdots (3.8\sqrt{\epsilon_r})/\text{h}$, in e.g. 20 intermediate steps.)

dielectric ridge guide where the lateral shield distance is $a = 100$ h. These curves are considered to verify the absorbing boundary formulations made for the 2-D FD-TD method.

As an example for open structures, Fig. 5 presents the E_{11}^y-mode dispersion curves for a dielectric guide. A graded mesh was used with a mesh ratio for the dielectric kernel (ϵ_{r1}) to the outer region of 1 to 5. The normalized dispersion curves, $B = [(\beta/k_0)^2 - 1]/(\epsilon_{r1} - 1)$ versus $V = k_0 a\sqrt{\epsilon_{r1} - 1}$, are plotted for different discretizations: 1 (8 × 16), 2 (16 × 32), 3 (40 × 80). The absorbing boundary is located in a distance of $5a/2$. The comparison with the FD frequency domain method [14] for the shielded dielectric waveguide (shield distance $100a$) demonstrates good agreement with the discretization case number 3.

Fig. 6 shows the EH_0- and HE_1-mode normalized propagation factor as a function of frequency for a realistic mm-wave shielded coplanar line with finite metallization thickness. Due to the finite thickness included in the 2-D FD-TD method, there are slight deviations in comparison with own calculations by the spectral domain approach (SDA) for $t = 0$. Two slot widths w_1 and w_2 are included in the calculations in order to demonstrate the flexibility of the method also for varying typical structure dimensions.

In principle, the limitations of the applicability of the method—like for all time domain methods—are given by the limited storage and cpu time capabilities of the computer and by the fact of decreasing accuracy concerning the propagation factors of the higher-order modes with

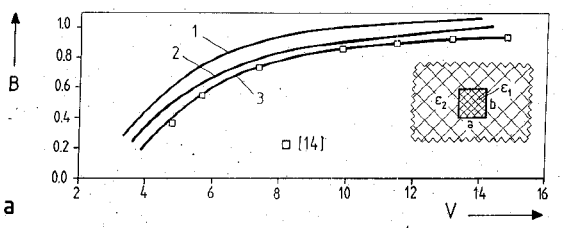

Fig. 5. Open dielectric guide $a = b$, $\epsilon_1 = 13.1\ \epsilon_0$, $\epsilon_2 = \epsilon_0$. Normalized dispersion curves of the E_{11}^y-mode, $B = [(\beta/k_0)^2 - 1]/(\epsilon_{r1} - 1)$ versus $V = k_0 a\sqrt{\epsilon_{r1} - 1}$, of the single dielectric waveguide for different discretizations: 1 (8 × 16), 2 (16 × 32), 3 (40 × 80). Comparison with the FD frequency domain method [14] for the shielded dielectric waveguide, shield distance 100a. Absorbing boundary in distance $5a/2$. Number of iterations $N_i = 2000$. Graded mesh ratio for the dielectric kernel: 1:5. (Choice of the propagation constant: $\beta = 2/a \cdots 15/a$, in e.g. 20 intermediate steps.)

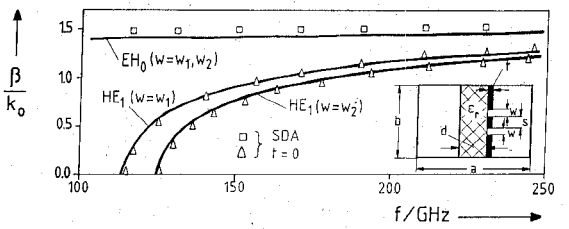

Fig. 6. EH_0- and HE_1-mode normalized propagation factor for the shielded coplanar line with finite metallization thickness t for different slot widths $w = w_1, w_2$. (For EH_0, the two curves are identical within the drawing accuracy of this figure.) Dimensions: $a = 0.8636$ mm, $b = 0.4318$ mm, $s = 0.072$ mm, $d = 0.126$ mm, $t = 0.018$ mm, $\epsilon_r = 3.7$, $w_1 = 0.09$ mm, $w_2 = 0.144$ mm. Discretization: 96 × 24. Number of iterations $N_i = 2000$. Comparison with own calculations with the Spectral Domain Approach (SDA) for $t = 0$. (Choice of the propagation constant: $\beta = 0 \cdots 7800$ 1/m, in e.g. 20 intermediate steps.)

increasing order. The computer requirements, however, are significantly reduced by utilizing the 2-D FD-TD method described in this paper and by introducing a graded mesh.

A shielded and a lateral open microstrip line is calculated in Fig. 7. The influence of the lateral shield on the expanded normalized propagation factor ratio $B\ [\%] = 100 \cdot (\sqrt{\epsilon_r} - (\beta/k_0))/\sqrt{\epsilon_r}$ as a function of frequency is demonstrated for typical dimensions for mm-wave applications. For a distance c with more than about ten times the half strip width, the influence of the lateral shield becomes negligible and tends to values obtained with the lateral absorbing boundary (curves 4, 5).

The 2-D FD-TD method presented in this paper may be utilized to calculate the characteristic impedance. After performing the Fourier transformation at the corresponding modal frequency, in each point of the mesh, the complete set of electric and magnetic field components is obtained. Dependent from the chosen definition of the characteristic impedance, the related integration can be carried out numerically. This procedure has already successfully been tested for the shielded microstrip line by using the voltage-current definition. Because this topic would be beyond the scope of this paper, results will be presented in a further paper.

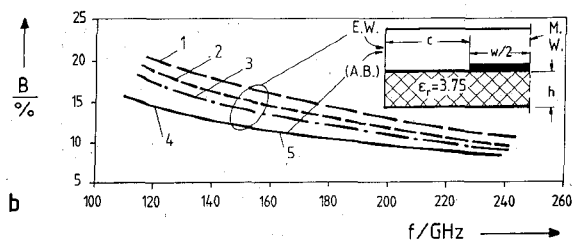

Fig. 7. Shielded and lateral open microstrip line. Influence of the lateral shield on the expanded normalized propagation factor ratio B [%] = 100 · $(\sqrt{\epsilon_r} - (\beta/k_0))/\sqrt{\epsilon_r}$ as a function of frequency for a single microstrip line. Dimensions: w = 0.16 mm, height b = 0.192 mm, ϵ_r = 3.7, h = 0.128 mm. Shield distances c: 1 (c = 0.248 mm ≙ 31Δl), 2 (c = 0.328 mm ≙ 41Δl), 3 (c = 0.408 mm ≙ 51Δl), 4 (c = 1.28 mm ≙ 160Δl). 5: Lateral open structure (curves 4 and 5 are identical within the drawing accuracy of Fig. 7.) (Choice of the propagation constant: ß = 3800 · · · 9800 1/m, in e.g. 20 intermediate steps.)

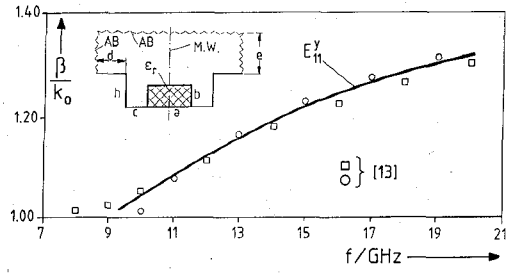

Fig. 8. Open trapped image guide. E^y_{11}-mode normalized propagation factor as a function of frequency. Dimensions: $a = b = c$ = 6 mm, h = 7 mm, ϵ_r = 2.23. Discretization: 54 × 42. Distance of the absorbing boundaries d = 6 mm, e = 7 mm. Number of iterations N_i = 1200. Comparison with [13]: □ □ □ combined effective dielectric constant transverse resonance method, ○ ○ ○ effective dielectric constant method. (Choice of the propagation constant: ß = 200 · · · 550 1/m, in e.g. 20 intermediate steps.)

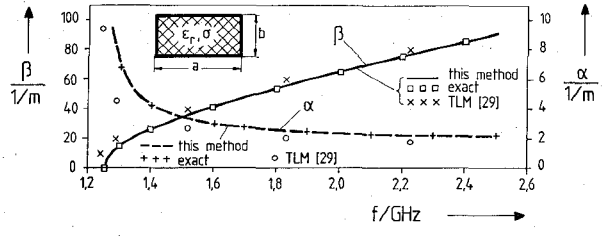

Fig. 9. Waveguide filled with a lossy dielectric. Attenuation factor α and propagation factor ß as a function of frequency. Comparison with the TLM method results (○ ○ ○, × × ×) of [33] and with the exact results (+ + +, □ □ □) obtained analytically. Parameters: a = 60 mm, b = 40 mm, ϵ_r = 4, σ = 0.02 S/m. Discretization: 30 × 40. Number of iterations N_i = 8000. (Choice of the propagation constant: ß = 0 · · · 90 1/m, in e.g. 20 intermediate steps.)

Fig. 8 shows the E^y_{11}-mode normalized propagation factor as a function of frequency for the open trapped image guide. The results compare well with those calculated in [13] with the transverse resonance effective dielectric constant techniques.

As an example where exact results are available, a waveguide filled with a lossy dielectric is investigated in Fig. 9. The attenuation factor α and propagation factor ß calculated with our method as a function of frequency are compared with the TLM method results of [33] and with the exact results obtained analytically. The curves in Fig. 9 verify the presented FD-TD method also for lossy structures by excellent agreement with the exact results.

Conclusion

A very efficient finite-difference time-domain formulation is presented for the full-wave analysis of shielded or open waveguiding structures. Lossy dielectrics and/or lossy conductors are included in the theory. This method utilizes advantageously a two-dimensional instead of the original three-dimensional Yee's mesh combined with adequately formulated absorbing boundary conditions and a graded mesh structure. The algorithm leads to a significant reduction in cpu time and storage requirements as compared with the conventional three-dimensional eigenvalue FD-TD mesh formulation and allows the inclusion of nearly arbitrarily shaped, fully or partially lateral open or shielded guiding structures with or without layers of finite metallization thickness. Dispersion characteristic examples for structures suitable for usual integrated circuits, such as insulated image guides, ridge guides, dielectric waveguides, trapped image guides, coplanar-lines, and microstrip lines elucidate the usefulness of the method. The theory is verified by comparison with results available from other methods.

References

[1] W. V. McLevidge, T. Itoh, and R. Mittra, "New waveguide structures for millimeter-wave and optical integrated circuits," *IEEE Trans. Microwave Theory Tech.*, vol. MTT-23, pp. 788–794, Oct. 1975.

[2] R. M. Knox "Dielectric waveguide microwave integrated circuits—An overview," *IEEE Trans. Microwave Tech.*, vol. MTT-24, pp. 806–814, Nov. 1976.

[3] J. A. Paul and Y.-W. Chang, "Millimeter wave image-guide integrated passive devices," *IEEE Trans. Microwave Theory Tech.*, vol. MTT-26, pp. 751–754, Oct. 1978.

[4] T. Itoh, "Open guiding structures for mmW integrated circuits," *Microwave J.*, pp. 113–126, Sept. 1982.

[5] S. E. Miller, "Integrated optics: An introduction," *Bell Syst. Tech. J.*, vol. 48, pp. 2059–2069, Sept. 1969.

[6] R. M. Knox and P. D. Toulios, "Integrated circuits for the millimeter through optical frequency range," in *Proc. Symp. Submillimeter Waves*, New York, May 1970, pp. 497–516.

[7] R. M. Knox, "Dielectric waveguides: A low-cost option for IC's," *Microwaves*, pp. 56–64, Mar. 1976.

[8] M. Ikeuchi, H. Swami, and H. Niki, "Analysis of open-type dielectric waveguides by the finite element iterative method," *IEEE Trans. Microwave Theory Tech.*, vol. MTT-29, pp. 234–239, Mar. 1981.

[9] N. Deo and R. Mittra, "A technique for analyzing planar dielectric waveguides for millimeter wave integrated circuits," *Arch. Elek. Übertragung*, vol. 37, pp. 236–244, July/Aug. 1983.

[10] U. Crombach, "Analysis of single and coupled rectangular dielectric waveguides," *IEEE Trans. Microwave Theory Tech.*, vol. MTT-29, pp. 870–874, Sept. 1981.

[11] B. M. A. Rahman and J. B. Davies, "Finite-element solution of integrated optical waveguides," *J. Lightwave Technol.*, vol. LT-2, pp. 682–687, Oct. 1984.

[12] S. M. Saad, "Review of numerical methods for the analysis of arbitrarily-shaped microwave and optical dielectric waveguides," *IEEE Trans. Microwave Tech.*, vol. MTT-33, pp. 894–899, Oct. 1985.

[13] W.-B. Zhou, and T. Itoh, "Analysis of trapped image guides using effective dielectric constant and surface impedances," *IEEE Trans. Microwave Theory Tech.*, vol. MTT-30, pp. 2163–2166, Dec. 1982.

[14] K. Bierwirth, N. Schulz, and F. Arndt, "Finite-difference analysis of rectangular dielectric waveguide structures," *IEEE Trans. Microwave Theory Tech.*, MTT-34, pp. 1104–1114, Nov. 1986.

[15] T. K. Sarkar, M. Manela, V. Narayanan, and A. R. Djordjevic, "Finite difference frequency-domain treatment of open transmission structures," *IEEE Trans. Microwave Theory Tech.*, vol. 38, pp. 1609–1616, Nov. 1990.
[16] T. Itoh, "Overview of quasi-planar transmission lines," *IEEE Trans. Microwave Theory Tech.*, vol. 37, pp. 275–280, Feb. 1989.
[17] M. Celuch-Marcysiak, W. K. Gwarek, "Formal equivalence and efficiency comparison of the FD-TD, TLM and SN methods in application to microwave CAD programs," in *Proc. European Microwave Conf.*, Stuttgart, Sept. 1991, pp. 199–204.
[18] K. S. Yee, "Numerical solution of initial boundary value problems involving Maxwell's equations on isotropic media," *IEEE Trans. Antennas Propagat.*, vol. AP-14, pp. 302–307, May 1966.
[19] A. Taflove, and M. E. Brodwin, "Numerical solution of steady state electromagnetic scattering problems using the time dependent Maxwell's equations," *IEEE Trans. Microwave Theory Tech.*, vol. MTT-23, pp. 623–630, Aug. 1975.
[20] G. Mur, "Absorbing boundary conditions for the finite-difference approximation of the time-domain electromagnetic-field equations," *IEEE Trans. on Elect. Compatibility*, vol. EMC-23, pp. 377–382, Nov. 1981.
[21] D. H. Choi, and W. J. R. Hoefer, "The finite-difference time-domain method and its applications to eigenvalue problems," *IEEE Trans. Microwave Theory Tech.* vol. MTT-34, pp. 1464–1470, Dec. 1986.
[22] W. Gwarek, "Analysis of arbitrarily shaped two-dimensional microwave circuits by finite-difference time-domain method," *IEEE Trans. Microwave Theory Tech.*, vol. 36, pp. 738–744, Apr. 1988.
[23] G.-C. Liang, Y.-W. Liu, and K. K. Mei, "Full-wave analysis of coplanar waveguide and slotline using the time-domain finite-difference method," *IEEE Trans. Microwave Theory Tech.*, vol. 37, pp. 1949–1957, Dec. 1989.
[24] D. M. Sheen, S. A. Ali, M. D. Abouzahra, and J. A. Kong, "Application of the three-dimensional time-domain method to the analysis of planar microstrip circuits," *IEEE Trans. Microwave Theory Tech.*, vol. 38, pp. 849–857, July 1990.
[25] M. Rittweger, M. Abdo, and I. Wolff, "Full-wave analysis of coplanar discontinuities considering three-dimensional bond wires," in *IEEE MTT-S Int. Symp. Dig.*, June 1991, pp. 465–468.
[26] D. H. Choi and W. J. R. Hoefer, "A graded mesh FD-TD algorithm for eigenvalue problems," in *Proc. European Microwave Conf.*, Rome, Sept. 1987, 413–417.
[27] Z. Chen, M. M. Ney, and W. J. R. Hoefer, "A new finite-difference time-domain formulation and its equivalence with the TLM symmetrical condensed node," *IEEE Trans. Microwave Theory Tech.*, vol. 39, Dec. 1991, pp. 2160–2169.
[28] I. S. Kim, and W. J. R. Hoefer, "A local mesh refinement algorithm for the time domain-finite difference method using Maxwell's curl equations," *IEEE Trans. Microwave Theory Tech.*, vol. 38, pp. 812–815, June 1990.
[29] H. Jin, R. Vahldieck, and S. Xiao, "An improved TLM full-wave analysis using a two dimensional mesh," in *IEEE MTT-S Int. Microwave Symp. Dig.*, July 1991, pp. 675–677.
[30] F. Arndt, V. J. Brankovic, and D. V. Krupezevic, "An improved FD-TD full wave analysis for arbitrary guiding structures using a two-dimensional mesh," in *IEEE MTT-S Int. Microwave Symp. Dig.*, 1992.
[31] N. R. S. Simons and E. Bridges, "Equivalence of propagation characteristics for the transmission-line matrix and finite-difference time-domain methods in two dimensions," *IEEE Trans. Microwave Theory Tech.*, vol. 39, pp. 354–357, Feb. 1991.
[32] J. S. Nielsen, and W. J. R. Hoefer, "Modification of the condensed 3-D TLM node to improve modeling of conductor edges," *IEEE Microwave Guided Wave Lett.*, vol. 2, pp. 105–110, Mar. 1992.
[33] H. Jin, R. Vahldieck, and S. Xiao, "A full-wave analysis of arbitrary guiding structures using a two-dimensional TLM mesh," in *Proc. European Microwave Conf.*, Stuttgart, pp. 205–210, Sept. 1991.

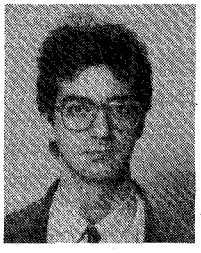

Veselin J. Brankovic was born in Zajecar, Yugoslavia, in 1964. He received the Dipl.-Ing. degree in electrical engineering from the University of Belgrade, Yugoslavia, in 1989.

Since 1990, he has been a Research Assistant at Microwave Department of the University of Bremen, Germany, where he is currently working toward the Ph.D. degree. His research activities include analysis of mm-wave structures using time domain numerical methods.

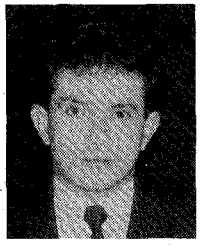

Dragan V. Krupezevic was born in Pozarevac, Yugoslavia, in 1964. He received the Dipl.-Ing. degree in electrical engineering from the University of Belgrade, Yugoslavia, in 1989.

Since 1991 he has been a Research Assistant at Microwave Department of the University of Bremen, Germany, where he is currently working toward the Ph.D. degree. His research interests include computational modeling of electromagnetic wave propagation using the Finite-Difference Time-Domain Method.

Fritz Arndt (SM'83) received the Dipl. Ing., Dr. Ing., and Habilitation degrees from the Technical University of Darmstadt, Germany, in 1963, 1968, and 1972, respectively.

From 1963 to 1972, he worked on directional couplers and microstrip techniques at the Technical University of Darmstadt. since 1972, he has been a Professor and Head of the Microwave Department of the University of Bremen, Germany. His research activities are in the area of the solution of field problems of waveguide, finline, and optical waveguide structures, of antenna design, and of scattering structures.

Dr. Arndt is member of the VDE and NTG (Germany). He received the NTG award in 1970, the A. F. Bulgin Award (together with three coauthors) from the Institution of Radio and Electronic Engineers in 1983, and the best paper award of the antenna conference JINA 1986 (France).